



Deposited via The University of Leeds.

White Rose Research Online URL for this paper:

<https://eprints.whiterose.ac.uk/id/eprint/677/>

Article:

Wong, K.K. and O'Farrell, T. (2003) Spread spectrum techniques for indoor wireless IR communications. *IEEE Wireless Communications*, 10 (2). pp. 54-63. ISSN: 1536-1284

<https://doi.org/10.1109/MWC.2003.1196403>

Reuse

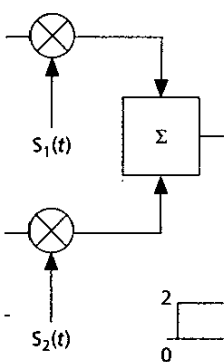
See Attached

Takedown

If you consider content in White Rose Research Online to be in breach of UK law, please notify us by emailing eprints@whiterose.ac.uk including the URL of the record and the reason for the withdrawal request.

SPREAD SPECTRUM TECHNIQUES FOR INDOOR WIRELESS IR COMMUNICATIONS

K. K. WONG AND TIM O'FARRELL, UNIVERSITY OF LEEDS



The DSSS solution for IR wireless transmission demonstrates that a transmission waveform can be designed to remove the key channel impairments in a wireless IR system.

ABSTRACT

Multipath dispersion and fluorescent light interference are two major problems in indoor wireless infrared communications systems. Multipath dispersion introduces intersymbol interference at data rates above 10 Mb/s, while fluorescent light induces severe narrowband interference to baseband modulation schemes commonly used such as OOK and PPM. This article reviews the research into the application of direct sequence spread spectrum techniques to ameliorate these key channel impairments without having to resort to complex signal processing techniques. The inherent properties of a spreading sequence are exploited in order to combat the ISI and narrowband interference. In addition, to reduce the impact of these impairments, the DSSS modulation schemes have strived to be bandwidth-efficient and simple to implement. Three main DSSS waveform techniques have been developed and investigated. These are sequence inverse keying, complementary sequence inverse keying, and M -ary bi-orthogonal keying (MBOK). The operations of the three systems are explained; their performances were evaluated through simulations and experiments for a number of system parameters, including spreading sequence type and length. By comparison with OOK, our results show that SIK, CSIK, and MBOK are effective against multipath dispersion and fluorescent light interference because the penalties incurred on the DSSS schemes are between 0–7 dB, while the penalty on OOK in the same environment is more than 17 dB. The DSSS solution for IR wireless transmission demonstrates that a transmission waveform can be designed to remove the key channel impairments in a wireless IR system.

INTRODUCTION

Wireless communications is focused on the delivery of high data rates. The engine that drives this paradigm is the requirement for wireless broadband services, and is underpinned by the explosive growth of IP technologies in recent years. Services ranging from Web browsing to multimedia, video streaming to fast packet transfer are creating the requirement for wireless

communication infrastructure that can support ever increasing data rates. Leading the field in the provision of high-speed wireless connectivity are technologies such as wireless LANs (WLANs), wireless personal area networks (WPANs), and wireless WANs (WWANs). In the radio domain, WLAN products based on the IEEE802.11b and 802.11a standards have become widespread in office, home, and public places due to their convenient usage model, reliability, and reduced cost. For WPAN applications, there are Bluetooth and the IEEE802.15.3 standard. In WWANs, third-generation (3G) mobile in the form of the 3G Partnership Project (3GPP) and 3GPP2 standards will be capable of supporting data rates up to 2 Mb/s. With research on 4G cellular mobile technologies starting, there remains an emphasis on higher data rate delivery.

Indoor wireless networking using infrared (IR) technology was first proposed over 20 years ago [1] and has now become a commercial reality. In 1993, the Infrared Data Association (IrDA) standard was established to create and promote interoperable low-cost IR data interconnection standards that support a point-to-point user model. The IrDA serial physical layer adopts on-off keying (OOK) with return-to-zero pulses for 1.152 Mb/s and 4-pulse position modulation (PPM) for 4 Mb/s serial links (www.irda.org) while very fast IR (VFIr) increases IrDA data rates to 16 Mb/s. The IrDA point-and-shoot usage model provides a simple usage context and implicit transmission security, which lead to wide acceptance in point-of-sales applications. The IEEE 802.11b WLAN standard also specifies an IR physical layer for diffuse transmission using 4- and 16-PPM to support 1 and 2 Mb/s rates, respectively [2]. Commercial realization of this standard has not progressed, and other than a small number of proprietary telepoint and diffuse IR systems capable of data rates up to 10 Mb/s, the number of deployed commercial point-to-multipoint IR systems is small. In contrast, research into high-data-rate IR wireless communication is substantial [3], covering the three key areas of devices, coding/modulation, and packet protocols. Collectively, such an ongoing research effort offers enormous potential to establish IR as a high-data-rate transmission medium complementing its radio counterpart.

The purpose of this article is to review recent research into the application of direct sequence spread spectrum (DSSS) in high-data-rate indoor wireless IR communication. The phenomenal success of spread spectrum in modern radio communications, noticeably IEEE802.11b, cellular code-division multiple access (CDMA), and ultra wideband (UWB), strongly motivates its use in an IR wireless context and hence its review here. The rationale for adopting a DSSS solution in the IR medium is argued. We give an overview of the nature of the IR channel and the main channel impairments. The fundamentals of sequence inverse keying (SIK), complementary SIK (CSIK), and M -ary bi-orthogonal keying (MBOK) for IR systems, which is a mapping of DSSS using bipolar spreading sequences into the IR (unipolar) medium, and their behavior in multipath propagation and artificial light interference are explained. We present the performance of these DSSS systems compared to OOK. Finally, concluding remarks are given.

WHY USE SPREAD SPECTRUM

The key advantages of indoor IR wireless communications are virtually unlimited bandwidth, compatible worldwide, and inherent security due to the confinement of IR signals within rooms. However, like radio channels, a transmitted signal in the IR channel can undergo multiple reflections before reaching the receiver. The resulting intersymbol interference (ISI) is a primary impediment to high-speed IR wireless transmission. Most attempts to resolve impairments caused by multipath propagation have focused on the use of equalization, angular, and imaging diversity [4–6]. Each of these solutions has its advantages and disadvantages, and their effectiveness depends on the modulation scheme used. Research has shown that the luminous flux produced by fluorescent lighting is not constant in time, but shows large fluctuations and fast variations in time [7]. Interference due to time variations in the power of the light is potentially detrimental to IR systems [8, 9]. Electrical high pass filtering is typically used to remove the interference produced by fluorescent lamps since the electrical spectrum of the interference is concentrated in the low-frequency region. However, the removal of the low-frequency components causes baseline wander in simple baseband systems. An alternative is to employ line coding schemes with small spectral content at low frequencies such as Manchester coding.

Although the exact nature of these impairments differ in the IR channel from the radio case, fundamentally they behave the same. Thus, DSSS techniques, which have been successfully used in radio systems to combat the same impairments, can be beneficially applied in indoor wireless IR systems. DSSS offers a transmission waveform that exploits the properties of a spreading sequence to resolve multipaths in an IR channel without having to resort to relatively complex solutions such as equalization, coded modulation, or elaborate optical frontends. In radio systems, DSSS uses bipolar

spreading sequences that cannot be used as such in the all-positive (unipolar) IR medium. This limitation was first removed in [10] by introducing the notion of unipolar-bipolar sequencing that allows the same spreading codes of radio systems to be used in optical systems. Originally, the technique was proposed for optical fiber CDMA LANs to:

- Remove the degradation caused by jumps in the DC level when multiple users randomly access the shared channel
- Offer larger code sets and smaller multiple access interference than unipolar codes (e.g., optical orthogonal or prime codes) of the same spreading factor

Unipolar-bipolar sequencing, which involves transmission of a unipolar spreading sequence and correlation with a bipolar version of the same spreading sequence, preserves the correlation properties of bipolar-bipolar sequencing, albeit with the introduction of a fixed dc offset unless balanced spreading sequences are used. In an IR channel, this means that unipolar-bipolar sequencing can resolve and suppress ISI caused by multipath propagation, and attenuate narrowband interference in a manner similar to that in a DSSS radio system. The full potential of unipolar-bipolar sequencing is exploited best in a multi-user system when more than one user accesses the IR channel simultaneously. In practice, most DSSS wireless IR systems limit channel access to a single user at a time; therefore, the photodetector can be ac-coupled to the preamplifier, thus obviating the need for balanced spreading sequences.

NATURE OF THE IR CHANNEL

In indoor wireless IR links, the most viable modulation and demodulation for an IR wireless system is intensity modulation and direct detection (IM/DD). In IM, information is carried by the intensity or power of the transmitted lightwave, not by its frequency or phase. In the DD technique, the photodiode produces a current that is proportional to the optical power incident upon it. An IR channel with IM/DD can be modeled as a baseband linear system [5, 6] expressed in Eq. 1, where $X(t)$ is the transmitted IR signal, $Y(t)$ is the current produced by the photodiode, which is proportional to the sum of the instantaneous optical power incident upon the photodiode surface, $h(t)$ is the channel impulse response, R is the photodiode responsivity, and $n(t)$ represents the shot noise generated in the photodiode.

$$Y(t) = \int_{-\infty}^{\infty} RX(\tau)h(t-\tau)d\tau + n(t) \quad (1)$$

In a receiver with a well designed preamplifier, the shot noise induced by ambient light such as sunlight and incandescent light is often the dominant noise source¹ [5, 7]. The power of the ambient light is typically much higher than that of the received signal; hence, the shot noise generated by this process can be considered independent of $X(t)$. Due to its high intensity, the shot noise is modeled as a zero-mean white Gaussian noise with double-sided power spectral density (PSD) $N_0/2 = qI_B$ where q is the charge

The key advantages of indoor IR wireless communications are virtually unlimited bandwidth, compatible worldwide, and inherent security due to the confinement of IR signals within rooms. However, like radio channels, a transmitted signal in the IR channel can undergo multiple reflections before reaching the receiver.

¹ Photodiode shot noise is also produced by the incident signal and the photodiode dark current, but the level is usually small compared to the ambient light induced shot noise.

The multipath signals arriving at the receiver at different time delays and with different powers results in pulse spreading which can cause severe power penalties at data rates above 10 Mb/s. The maximum transmission speed ultimately depends on the relative distance between the transceivers and the size of the room.

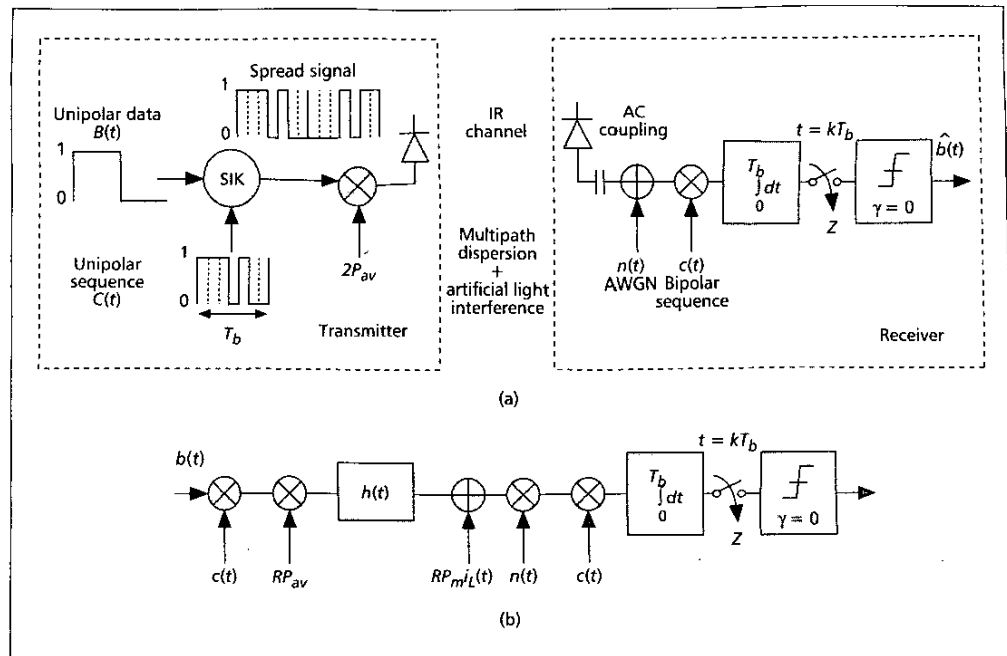


Figure 1. Modeling of an IR wireless SIK system. a) unipolar-bipolar sequencing b) ac-coupled SIK system with equivalent channel.

of an electron and I_b is the dc photocurrent proportional to the ambient light power. The optical spectrum of the ambient light extends from 400 nm up to 1500 nm, covering the 780–950 nm band of interest for low-cost IR systems. Optical filtering is often used to remove ambient light outside the transmitted signal bandwidth.

IR systems differ from conventional radio systems in several aspects. The channel input $X(t)$ represents instantaneous optical power, not the amplitude of the electric field. Hence, $X(t)$ must be nonnegative, and the average transmitted optical power is given by the time average of $X(t)$. Multipath propagation causes the received electric field to undergo amplitude fades on the scale of an IR wavelength. However, the relative size of a photodiode is typically 10–100,000 times larger than the IR wavelength. As the current $Y(t)$ is proportional to the integral of the square of the electric field over the entire photodiode surface, this leads to spatial diversity that prevents multipath fading [4, 5].

MULTIPATH DISPERSION

Although there is no multipath fading, IR channels are still subject to multipath dispersion as a result of multipath propagation. Multipath signals arriving at the receiver at different time delays and with different powers result in pulse spreading, which can cause severe power penalties at data rates above 10 Mb/s. The maximum transmission speed ultimately depends on the relative distance between the transceivers and the size of the room [1]. Hence, modulation schemes that are robust to multipath dispersion will be more reliable at high data rates and for larger transceiver coverage. Fortunately, multipath dispersion is completely characterized by the channel impulse response. Characterization of

the multipath channel response through experimental measurements [11] using a swept-modulation frequency technique found that the channel response is very dynamic, exhibiting large variations between channels in different rooms, and also between channels with different transmitter and receiver locations and orientations in the same room. Measurements show that reflected signals can contain significant energy up to 70 ns after the arrival of the LOS pulse. A useful measure of the severity of multipath dispersion is the channel root mean square delay spread, which represents the standard deviation of the delayed multipath signals.

FLUORESCENT LIGHT INTERFERENCE

The rapid fluctuations of the optical power produced by fluorescent lights manifests itself as interference. This interference has different intensity and bandwidth characteristics depending on the type of lamp that produced it. Based on the average irradiance and interference, the artificial light sources can be grouped into three classes and mathematically modeled in the form of Fourier series [7]:

- Incandescent lamps
- Fluorescent lamps with conventional ballasts
- Fluorescent lamps with electronic ballasts

Fluorescent lamps with conventional ballasts are driven at the power line frequency of 50 or 60 Hz, and their electrical spectra contain energy at harmonics up to tens of kilohertz. Fluorescent lamps with electronic ballasts are driven at tens of kilohertz, resulting in a detected electrical spectrum containing energy at harmonics of the drive frequency that can extend up to 1 MHz and above. This interference with a wide frequency occupancy presents a more serious impairment than conventional fluorescent lamps [8, 9].

DIRECT SEQUENCE SPREAD SPECTRUM INFRARED SYSTEM

This section describes the operation of SIK, CSIK, and MBOK and explains how multipath dispersion and fluorescent light interference are attenuated.

SEQUENCE INVERSION KEYING MODULATION

A schematic diagram of the transmitter and receiver of an SIK system is shown in Fig. 1a [12, 13]. At the transmitter, the unipolar data, $B(t)$ is used to sequence inverse key an unipolar spreading sequence, $C(t)$ such that the transmitted DSSS signal comprises $C(t)$ or its complement. The duration of N chips in one period of the spreading sequence is equal to the bit duration. The unipolar spread signal is scaled by $2P_{av}$ where P_{av} is the mean signal optical power. Alternatively, SIK modulation of $B(t)$ on $C(t)$ can be represented as the multiplication of the bipolar version of the data, $b(t)$, and the bipolar version of the spreading sequence $c(t)$, with a dc offset term added, $B(t) \otimes C(t) = [b(t)c(t) + q(t)]/2$, where \otimes denotes SIK and $q(t)$ is a constant unit amplitude signal.

During transmission through the channel, the spread signal undergoes multipath dispersion and is corrupted by fluorescent light interference. At the receiver, the detected photocurrent is high-pass filtered to remove the dc component. An equivalent simplified schematic diagram for an ac-coupled SIK system is illustrated in Fig. 1b. In a DSSS system, the spread signal has a large number of chip transitions within a data bit duration. The high transition rate of these chips significantly reduces the baseline wander effect due to ac-coupling and can be ignored in system bit error rate (BER) analysis. Despreading of the ac-coupled photocurrent is realized by multiplying directly with $c(t)$. The despread signal is integrated over one data bit duration T_b , sampled at T_b intervals to produce correlator output signal Z as given in Eq. 2, where β_l is the relative power of the l th resolved multipath, $C_c(l)$ is the aperiodic autocorrelation function (ACF) of the spreading sequence, l is the discrete time shift, P_m is the average power of the fluorescent light interference and $i_L(t)$ the zero-mean interference waveform, and n_o is the Gaussian noise component. Z is then fed to a threshold detector with the threshold level set to zero.

$$Z = RP_{av}\beta_0 b_0 + \frac{RP_{av}}{N} \sum_{l=1}^{L-1} \beta_l [b_{-1} C_c(1-N) + b_0 C_c(l)] + \frac{RP_m}{N} i_L(T_b) + n_o \quad (2)$$

Without interference and Gaussian noise, a positive Z means +1 was transmitted, and a negative Z that -1 was transmitted. The presence of interferences increases the probability of error in estimating $\hat{b}(t)$. The delayed multipath signals (i.e., the second term of Eq. 2) that are not synchronized with the receiver reference sequence are modulated by the previous data bit

b_{-1} and the present data bit b_0 over the integration interval. Since the data sequence is random, the delayed multipath signals may change sign during the integration interval. If there is no sign change (i.e., $b_{-1} = b_0$), the correlation of the multipath signal with the reference sequence equals the periodic ACF of the spreading sequence. By using an m -sequence as the spreading sequence, the power of the multipath signal would be reduced by a factor of N since an m -sequence has a periodic ACF of value $-1/N$ at a time shift greater than a chip duration. When $b_{-1} = -b_0$, the attenuation of the multipath signals would depend on the odd ACF of the m -sequence at the time shift corresponding to the delays of the multipath signals. However, the odd ACF of an m -sequence is not an impulse. In order to reduce the effect of multipath dispersion as much as possible, spreading sequences such as an m -sequence with odd ACF having the least sidelobe magnitudes should be used.

For DSSS systems with high chip rate, $i_L(t)$ fluctuates slowly with respect to the spreading sequence over the integration period and may be considered constant over the integration period. This constant value $i_L(T_b)$ in the third term of Eq. 2 is a random variable that depends on the sampled value of the interference waveform. This assumption simplifies the analysis of the fluorescent light interference component of Z , but is only valid when the data rate is larger than the periodicity of the highest harmonic of the interfering signal. A rule of thumb is 10 times greater. Viewed in the frequency domain, the fluorescent light interference behaves as a narrowband jammer in comparison to the bandwidth of a DSSS signal. The despreading process at the receiver restores the desired signal to its original bandwidth before spreading, and spreads the narrowband interfering signal to a bandwidth at least equal to the bandwidth of the spreading sequence, thus reducing the interference PSD. When the bandwidth of the integrator is equal to the data Nyquist bandwidth, the interference power at the integrator output is attenuated by the spreading factor compared to a nonspread system. In contrast, for OOK the interference adds directly to the OOK symbol, causing substantial distortion with respect to the fixed detection threshold, giving a high BER.

COMPLEMENTARY SEQUENCE INVERSE KEYING MODULATION

An earlier section shows that the performance of an SIK system in a multipath channel depends very much on the partial correlation properties of the spreading sequences used. CSIK is proposed to overcome this restriction [13]. A schematic diagram of the CSIK modulation scheme is illustrated in Fig. 2a. Figure 2b shows the inclusion of a cancellation filter, the function of which will be explained later. At the transmitter, the binary data bit sequence modulates a pair of binary complementary sequences (BCP) instead of an m -sequence. The modulated sequences are summed, and a dc offset P_{dc}

The despreading process at the receiver restores the desired signal to its original bandwidth before spreading, and spreads the narrowband interfering signal to a bandwidth at least equal to the bandwidth of the spreading sequence, thus reducing the interference PSD.

Though SIK and CSIK are tolerant to interference, a key reservation concerning the use of these systems is the spreading factor which limits the system bandwidth efficiency.

$= 2$ is added to ensure that the transmitted signal is positive at all times. The unipolar signal is then scaled by a factor of $P_{av}/2$ to obtain an average signal power of P_{av} . This process of adding a dc offset and scaling realizes a unipolar-bipolar sequencing scheme. At the receiver, despreading is achieved by multiplying by the same two (bipolar) sequences of the BCP, integrated over T_b duration and sampled at intervals of T_b to produce correlator outputs Z_1 and Z_2 , which are summed to produce Z as expressed in Eq. 3, and then fed to a detector with threshold set at zero.

$$Z = b_0 \beta_0 R P_{av} + \frac{R P_{av}}{2N} \sum_{j=1}^2 \left\{ \sum_{m=1}^2 \sum_{l=1}^{L-1} \beta_l \left[\begin{array}{l} [b_{-1} C_{S_m, S_j}] \\ (l-N)+ \\ [b_0 C_{S_m, S_j}(l)] \end{array} \right] \right\} + \frac{R P_{av} i_L(T_b)}{N} \sum_{j=1}^2 \sum_{n=0}^{N-1} S_{j,n} + \sum_{j=1}^2 n_j \quad (3)$$

Without interference and Gaussian noise, a positive Z means a +1 data is received while a negative Z means a -1 data is received. Similar

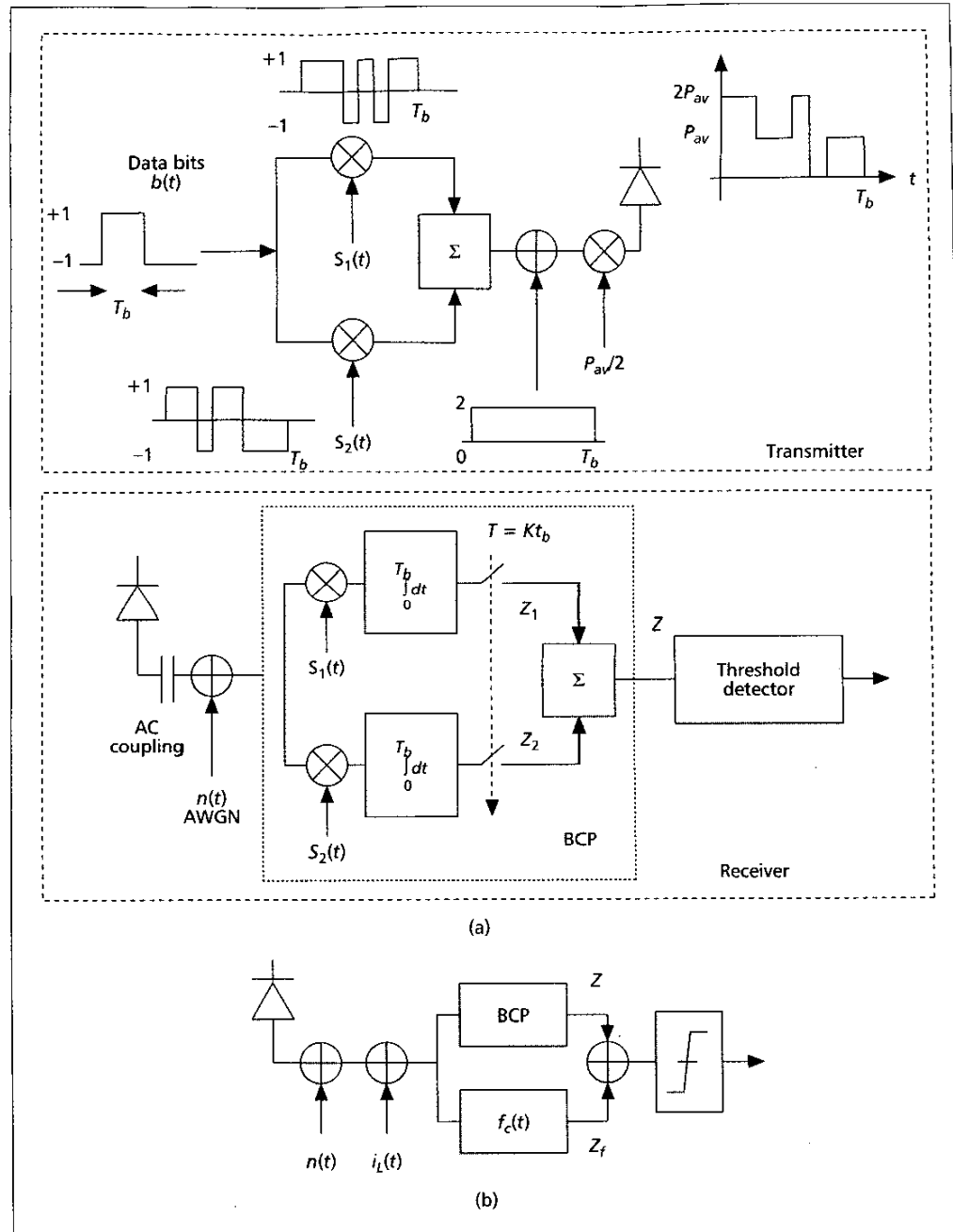


Figure 2. A schematic diagram of a CSIK system: a) a receiver without a cancellation filter; b) a receiver with a cancellation filter.

to SIK, multipath interference on Z depends on the partial correlations of the receiver reference sequences with the delayed versions of the transmitted sequence. However, due to the aperiodic autocorrelation properties of the sequences in a BCP, summation of Z_1 and Z_2 results in the sidelobes of the aperiodic AFCs and cross-correlation functions (CCFs) of the sequences in the second term of Eq. 3 canceling each other, hence creating zero correlation zones (ZCZs). Consequently, the multipath interference can be eliminated almost completely. The degree to which the multipath dispersion is reduced depends on the amounts by which the sidelobes of the aperiodic ACF and CCF are removed. In an IR channel this property can be exploited by arranging for constructive ISI to occur, thus enhancing the system performance [13]. The approximation of $i_L(t)$ to $i_L(T_b)$ in the third term of Z means that the interference effect depends on the total chip balance in the BCP.

M-ary BI-ORTHOGONAL KEYING MODULATION

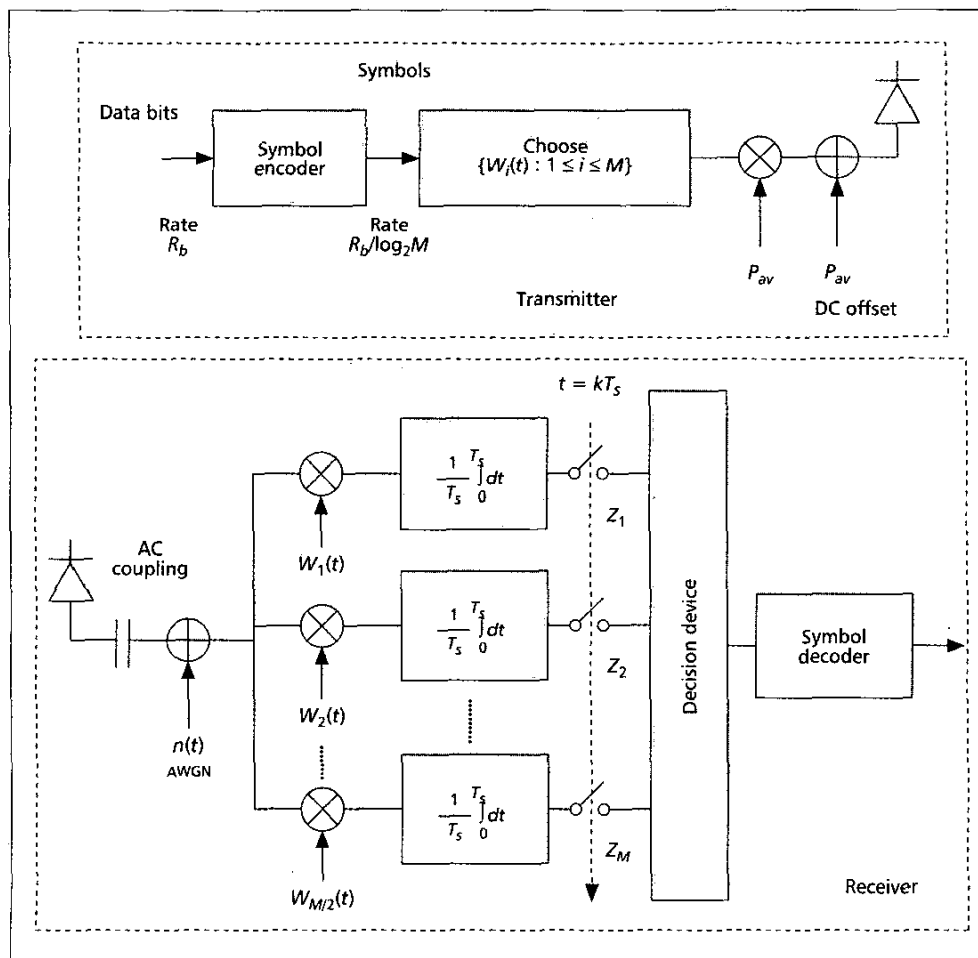
Though SIK and CSIK are tolerant of interference, a key reservation concerning the use of these systems is the spreading factor, which limits system bandwidth efficiency. A method for improving bandwidth and power efficiency is M -ary modulation. A DSSS system using MBOK

Room		Transmitter		Receiver	
Length (x)	10 m	x-coordinate	5 m	x-coordinate	1.25 m
Width (y)	10 m	y-coordinate	5 m	y-coordinate	1.25 m
Height (z)	3 m	z-coordinate	3 m	z-coordinate	0 m
Reflection coefficient	0.8	Elevation	-90°	Elevation	90°
		Azimuth	0°	Azimuth	0°
				Area	1 cm ²
				FOV	90°
				Responsivity	1 A/W

■ Table 1. The simulation parameters for the IR channel.

[14] improves power and bandwidth efficiency while retaining the beneficial properties of DSSS. In MBOK, $\log_2 M$ data bits per spreading sequence are transmitted, which lowers the chipping rate and consequently reduces the effect of multipath dispersion at the expense of system complexity.

A schematic diagram of an ac-coupled MBOK system is shown in Fig. 3. At the trans-



■ Figure 3. A schematic of an MBOK wireless IR system.

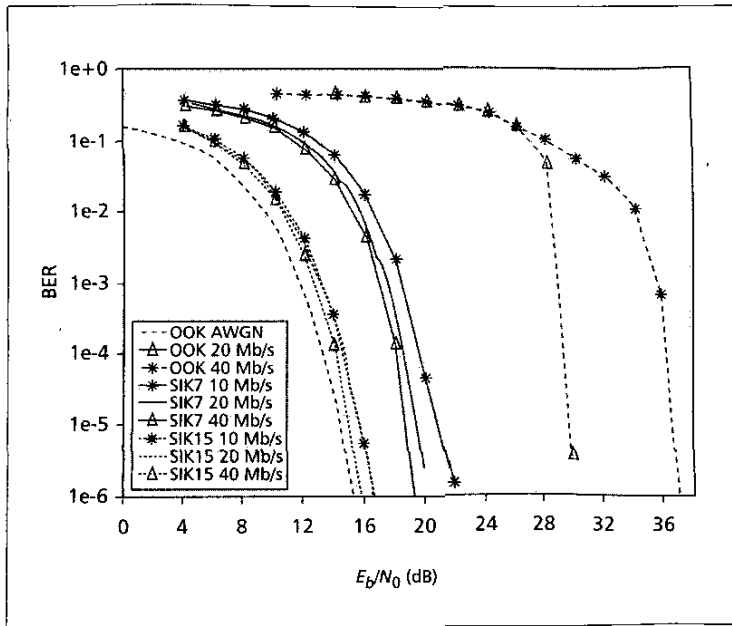


Figure 4. Simulated BER vs E_b/N_0 performance of SIK7 and SIK15 at 10, 20, and 40 Mb/s, and OOK at 20 and 40 Mb/s in the presence of multipath dispersion and 10 dB fluorescent light interference.

mitter, blocks of $k = \log_2 M$ binary data bits of rate $1/T_b$ are mapped onto symbols of rate $1/T_S = 1/(T_b \log_2 M)$. An orthogonal code consisting of $M/2$ orthogonal sequences of length N , $\mathbf{W}_{M/2,N}$ and the complements of $\mathbf{W}_{M/2,N}$ are used to represent the M equiprobable symbols. One easy way to obtain a set of orthogonal codes in which the $M/2$ orthogonal sequences are selected for MBOK is from the rows of a Hadamard matrix [15]. The receiver for an MBOK system requires only $M/2$ correlators. This is because in the absence of Gaussian noise and interference, the μ th correlator output, Z_μ , expressed in Eq. 4, produces $+RP_{av}\beta_0$ at the sampling time for a +

$W_\mu(t)$ sequence transmitted, or $-RP_{av}\beta_0$ for its complement, and zero for all the other sequences. Thus, only the positive $M/2$ code sequences $\mathbf{W}_{M/2,N}$ need to be generated at the receiver. The decision device then selects the correlator output with the largest magnitude (in this case the μ th symbol) and acquires the sign (positive or negative) information of this variable.

$$Z_\mu = RP_{av}\beta_0 + \frac{RP_{av}}{2N} \sum_{l=1}^{L-1} \beta_l \left[C_{W_\gamma, W_\mu}(l-N) + C_{W_\gamma}(l) \right] + \frac{RP_m i_L(T_S)}{N} \sum_{n=0}^{N-1} W_{\mu,n} + n_o$$

In the presence of multipath dispersion, the multipath signal delayed by τ_l with respect to the receiver reference sequence carries the γ th symbol during the time interval $[\tau_l - T_S, \tau_l]$ and the μ th symbol during the time interval $[\tau_l, \tau_l + T_S]$ during the integration period of T_S . Since the data blocks that are grouped into symbols are random, there is a $1/M$ chance that γ and μ are equal. Hence, the performance of MBOK depends on the aperiodic ACF and CCF of the sequences in the set. The approximation of $i_L(t)$ by $i_L(T_S)$ and the use of soft decision decoding means that the effect of fluorescent light interference depends on the chip balance of each sequence in the set.

SIMULATION AND EXPERIMENTAL RESULTS

The BER vs. E_b/N_0 performances of SIK, CSIK, and MBOK under the influence of multipath dispersion and electronic ballast-driven fluorescent light interference are presented in this section. The simulation parameters for the nondirected line-of-sight (LOS) IR channel configuration used in the study are shown in Table 1 [13]. The multipath impulse response up to three

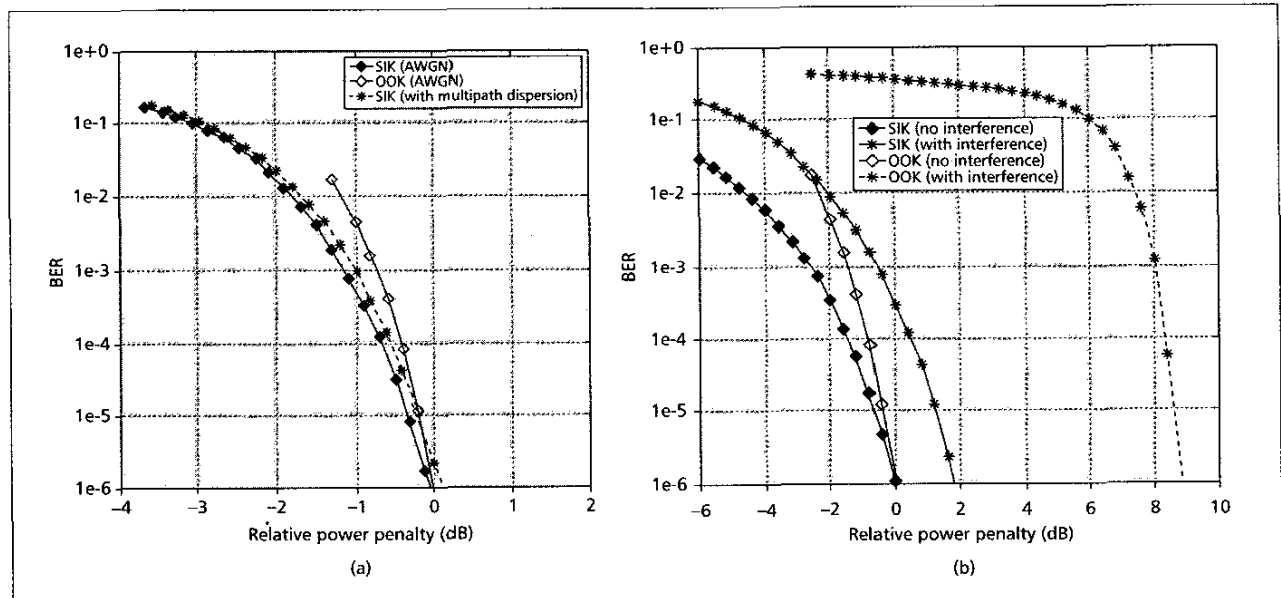


Figure 5. Experimental BER performance of SIK and OOK systems: a) with multipath dispersion; b) with fluorescent light interference.

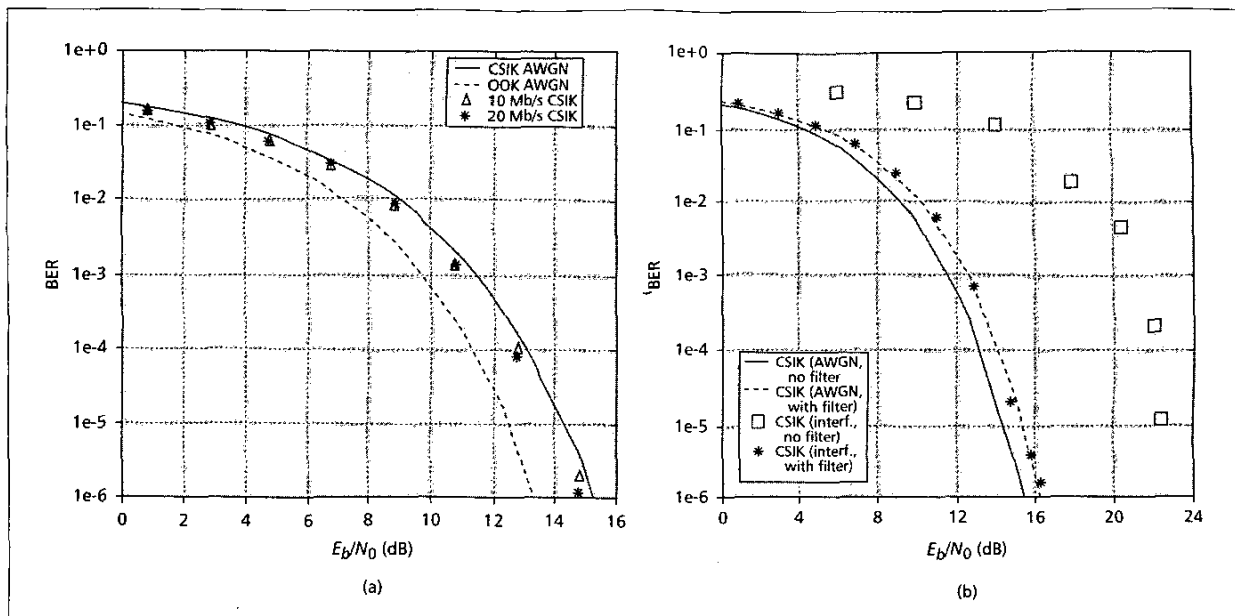


Figure 6. BER vs. E_b/N_0 performance for CSIK8: (a) at 10 and 20 Mb/s in the presence of multipath dispersion and exploiting constructive ISI; (b) with and without cancellation filter at 1 Mb/s in the presence of fluorescent light interference.

reflections is obtained using the simulation model in [16]. The relative power in the LOS path is normalized to unity, and the effects of path loss and shadowing are ignored. The average power of the fluorescent light interference is 10 times the average signal power. The results for OOK are included as a benchmark. All the systems have the same average signal power of P_{av} , and the power penalty incurred is defined as the E_b/N_0 (dB) difference at 10^{-6} BER between the system with interference and OOK in an additive white Gaussian noise (AWGN) channel only.

Note that in this comparative study, the DSSS IR systems and OOK systems have the same noise PSD as the shot noise at the receiver front-end is mainly due to ambient light with intensity much higher than that of the signal. A DSSS IR system with m -spreading factor increases the bandwidth at the receiver front-end by m times, and hence increases the noise by the same factor. However, as the bandwidth of the integrator is equal to that of the data, the noise power fed to the threshold detector is the same for both spread spectrum and OOK systems operating the same bit/symbol rate. That is, SIK and OOK have the same BER theoretical performance in AWGN.

Figure 4 shows the performance of SIK and OOK at 10, 20 and 40 Mb/s. M -sequences of lengths 7 (SIK7) and 15 (SIK15) are tested. The total power penalties of each SIK system do not differ much as the data rate varies, and decrease with increasing N . For SIK7, the penalties range from 6 to 8 dB while for SIK15, the penalties are about 4 dB. The performance of unequalized OOK in the same multipath channel is also plotted for comparison. The penalties for OOK are large (i.e., 17 dB at 20 Mb/s) and increases to 23 dB at 40 Mb/s. These results demonstrate the resilience of the spread spectrum technique

against multipath dispersion and fluorescent light interference. The weakness of OOK is attributable to the detection threshold, which is sensitive to the actual values of the interference levels. Even though SIK also uses a threshold detector, the much superior performance demonstrates the effectiveness of DSSS techniques against multipath dispersion and fluorescent lamp interference.

A 2 Mb/s IR wireless SIK testbed with a spreading factor of 31 was constructed to provide experimental BER results [12]. The SIK testbed can be converted to an OOK testbed by changing the m -sequence to an all 1 sequence to provide experimental OOK results in the same environment for comparison. Figure 5a shows the results with multipath dispersion only. The BER is plotted as a function of relative electrical power, where 0 dB corresponds to the receiver sensitivities for SIK (-42 dBm) and OOK (-45.7 dBm) at a BER of 10^{-6} , respectively. The penalty on SIK due to multipath dispersion is almost negligible (i.e., 0.1 dB). There is no degradation due to multipath dispersion for OOK at 2 Mb/s due to the low data rate. With the high spreading factor of SIK, there are resolved delay multipaths compared with OOK, but the impact on SIK is insignificant. Figure 5b shows the result for both SIK and OOK with electronic ballast fluorescent light interference. As the same known multipath ISI is inclusive in both cases, the relevant power penalty is due to interference only. With 10 dB of interference, the penalty incurred in SIK is only 1.8 dB, while the penalty on OOK was measured at 8.8 dB. The experimental results demonstrate the improvement offered by SIK over OOK when transmitting in the same amount of interference.

Figure 6a shows the simulation results for CSIK transmitting a BCP of length 8 (CSIK8) at 10 and 20 Mb/s. The solid line represents the

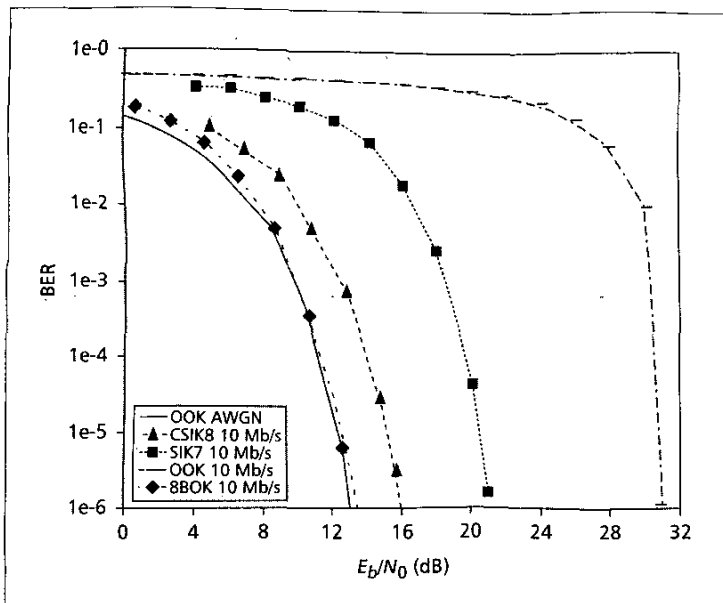


Figure 7. Comparing the BER vs E_b/N_0 performance of OOK, SIK7, CSIK8 (with cancellation filter), and 8-BOK at 10 Mb/s in the presence of multipath dispersion and fluorescent light interference.

performance in an AWGN channel, while the symbols represent the performance with multipath dispersion. CSIK suffers from an E_b/N_0 penalty of 1.76 dB compared to OOK or SIK in an AWGN channel. This is because the noise power is increased by having two correlators in the receiver. In the multipath channel, no BER degradation is seen even though the powers in the delayed paths are as high as 30–60 percent of the LOS path. Instead, there is a net improvement in the BER performance because of the ZCZ property described earlier.

The effect of the fluorescent light interference is determined by the total chip balance of the sequences in the BCP. A set of sequences is considered to be balanced if the sum of all the +1 chips and -1 chips of the sequences, denoted $\sum \Sigma s_{j,n}$, is equal to zero. In general, a BCP is not balanced, and as shown in Fig. 6b for a data rate of 1 Mb/s, this can lead to power penalties of 8 dB in fluorescent light interference with power five times the mean signal power. Typically, it is found that all data rates greater than 1 Mb/s show similar levels of degradation. This severe degradation can be reduced by adding a cancellation filter, $f_c(t)$ with the same period as the complementary sequences at the receiver, as shown in Fig. 2b [13]. If $\sum \Sigma s_{j,n}$ in the BCP is N , the sum of the coefficients of $f_c(t)$ should be $-N$ to cancel the fluorescent light interference component in Z and vice versa. In addition, the cancellation filter must strive to introduce minimum noise enhancement and multipath interference to Z . The performance of CSIK8 with cancellation filter $f_c(t) = \{-1, 0, 0, 0, 0, -1, -1, -1\}$ (in this case, $\sum \Sigma s_{j,n} = 4$) is also shown in Fig. 6b for a 1 Mb/s data rate. The effectiveness of the cancellation filters is evident as there is no degradation due to 10 dB of fluorescent light interference and negligible multipath dispersion. The E_b/N_0

penalty in an AWGN channel induced by the cancellation filter is about 1 dB.

Figure 7 compares the BER vs. E_b/N_0 performance of all the schemes, OOK, SIK7, CSIK8 (with cancellation filter), and 8BOK (i.e. $M = 8$) at a data rate of 10 Mb/s. The orthogonal code for 8-BOK uses length 8 sequences taken from the even-numbered rows of a Hadamard matrix and their complements. The respective power penalties with respect to OOK in AWGN only are 17.5 dB, 7.5 dB, 2.5 dB, and 0 dB, respectively. The results clearly demonstrate the effectiveness of the DSSS approach in the IR channel.

CONCLUSIONS

This article has reviewed three key DSSS techniques (SIK, CSIK, and MBOK) that can bring benefit to communication in the indoor wireless IR channel. Although the precise details of the methods differ from the radio case due to the unipolar nature of the IR (optical) channel, like the radio case the schemes benefit from the spreading sequence properties and processing gain advantage of DSSS. Typically, spreading sequences with small aperiodic auto- and cross-correlation sidelobes should be used in order to minimize ISI resulting from multipath propagation. This principle is taken to its limit in CSIK, where the use of complementary spreading sequences seeks to remove completely the sidelobes of the auto- and cross-correlation functions.

In order to minimize narrowband interference effects, balanced spreading sequences should be used. When this is not possible, interference cancellation filters can be designed to remove the interference component. The coefficients of the cancellation filters are chosen to minimize noise enhancement while at the same time minimizing the sidelobes of the cross-correlation function of the filter impulse response and the spreading sequences.

While SIK and CSIK successfully overcome multipath and interference impairments, opening the way for high-data-rate transmission, they are limited by the bandwidth of the optoelectronic interfaces, particularly at the receiver. In order to enhance the power and bandwidth efficiency, M -ary bi-orthogonal keying using orthogonal sets of spreading sequences is recommended. Like SIK and CSIK, MBOK benefits from using spreading sequences with small auto- and cross-correlation sidelobes and gives good performance in narrowband interference when balanced sequences are used.

The fundamental premise that major signal impairments in the IR medium can be overcome by the design of an appropriate transmit waveform is asserted by using DSSS techniques. This approach can play a key role in achieving low-complexity high-speed data rates for indoor wireless IR communication systems.

REFERENCES

- [1] F. R. Gfeller and U. Bapst, "Wireless In-House Data Communication via Diffuse Infrared Radiation," *Proc. IEEE*, vol. 67, Nov. 1979, pp. 1474–86.
- [2] R. T. Valadas et al., "The Infrared Physical Layer of the IEEE 802.11 Standard for Wireless Local Area Networks," *IEEE Commun. Mag.*, vol. 36, Dec. 1998, pp. 107–12.

- [3] K. Akhavan, M. Kavehrad, and S. Jivkova, "Wireless Infrared In-House Communications: How to Achieve Very High Bit Rates," *Proc. IEEE WCNC*, vol. 2, 200, pp. 698-703.
- [4] J. M. Kahn and J. R. Barry, "Wireless Infrared Communications," *Proc. IEEE*, vol. 85, 1997, pp. 265-98.
- [5] J. R. Barry, *Wireless Infrared Communication*, Kluwer, 1994.
- [6] P. Djahani and J. M. Kahn, "Analysis of Infrared Wireless Links Employing Multi-beam Transmitters and Imaging Diversity Receivers," *IEEE GLOBECOM*, vol. 1a, 1999, pp. 497-504.
- [7] A. J. C. Moreira, R. T. Valadas, and A. M. de Oliveira Duarte, "Optical Interference Produced by Artificial Light," *Wireless Networks*, vol. 3, 1997, pp. 131-40.
- [8] A. J. C. Moreira, R. T. Valadas, and A. M. de Oliveira Duarte, "Performance of Infrared Transmission Systems Under Ambient Light Interference," *IEE Proc. Optoelect.*, vol. 143, 1996, pp. 339-46.
- [9] R. Narashimhan, M. D. Audeh, and J. M. Kahn, "Effect of Electronic-Ballast Fluorescent Lighting on Wireless Infrared Links," *IEE Proc. Optoelect.*, vol. 143, 1996, pp. 347-54.
- [10] T. O'Farrell, "Code-division Multiple-access (CDMA) Techniques in Optical Fibre Local Area Networks," Ph.D. thesis, Manchester Univ., U.K., 1989.
- [11] J. M. Kahn, W. J. Krause, and J. B. Carruthers, "Experimental Characterization of Nondirected Indoor Infrared Channels," *IEEE Trans. Commun.*, vol. 43, 1995, pp. 1613-23.
- [12] K. K. Wong, T. O'Farrell, and M. Kiatweerasakul, "Infrared Wireless Communication using Spread Spectrum Techniques," *IEE Proc. Optoelect.*, vol. 147, Aug. 2000, pp. 308-14.
- [13] K. K. Wong, "Bandwidth Efficient Modulation Techniques for Spread Spectrum Based Wireless Infrared Transmission," Ph.D. thesis, Univ. of Leeds, U.K., 2002.
- [14] K. K. Wong and T. O'Farrell, "Biorthogonal Direct-Sequence Spread Spectrum System for Infrared Wireless Communications," *11th IEEE PIMRC*, London, U.K., 2000, pp. 933-38.

- [15] H. F. Harmuth, *Transmission of Information by Orthogonal Functions*, 2nd ed., Springer-Verlag, 1972.
- [16] J. R. Barry et al., "Simulation of Multipath Impulse Response for Indoor Wireless Optical Channels," *IEEE JSAC*, vol. 11, 1993, pp. 367-79.

BIOGRAPHIES

K. K. WONG (eenkkw@ecu-01.novell.leeds.ac.uk) received his B.Eng. (1st Class) and Ph.D. degrees in electronic and electrical engineering from the University of Leeds in July 1997 and March 2002, respectively. His Ph.D. work focused on the application of spread spectrum techniques to indoor infrared wireless communications. From December 2000 to December 2002 he worked as a research fellow at the School of Electronic and Electrical Engineering, University of Leeds, and investigated turbo coding and decoding, IEEE 802.11g WLAN, Bluetooth, and DECT. His research interests include infrared, spread spectrum, cellular mobile, and WLAN technologies. He is a member of the IEE.

TIM O'FARRELL [M] (t.ofarrell@ee.leeds.ac.uk) has been at the University of Leeds since 1996, where he is currently a senior lecturer of communications engineering. He leads a research team specializing in sequence, coding, and modulation techniques for broadband wireless communications. He holds a B.Sc. from Birmingham University, and M.Sc. and Ph.D. from Manchester University in electrical and electronic engineering. Previously, he worked in industry for Roke Manor Research, held academic posts at the Asian Institute of Technology and Manchester University, and has been a visiting research fellow at Sydney University. He has research interests in sequences, coding, and modulation for 3/4G mobile, WLANs, and infrared wireless communication, as well as radio resource management for 3G mobile. In 1999 he founded Supergold Communication Ltd., a startup company specializing in WLAN and 3G technology, and is now director of algorithm research. He is a Chartered Member of the IEE.

Like SIK and CSIK,
MBOK benefits from
using spreading
sequences with small
auto- and
cross-correlation
sidelobes and gives
good performance in
narrow band
interference when
balanced sequences
are used.